



**HAL**  
open science

# Identification of sources of potential fields with the continuous wavelet transform: Application to self-potential profiles

Dominique Gibert, Marc Pessel

► **To cite this version:**

Dominique Gibert, Marc Pessel. Identification of sources of potential fields with the continuous wavelet transform: Application to self-potential profiles. *Geophysical Research Letters*, 2001, 28 (9), pp.1863-1866. 10.1029/2000GL012041 . insu-03324637

**HAL Id: insu-03324637**

**<https://insu.hal.science/insu-03324637>**

Submitted on 23 Aug 2021

**HAL** is a multi-disciplinary open access archive for the deposit and dissemination of scientific research documents, whether they are published or not. The documents may come from teaching and research institutions in France or abroad, or from public or private research centers.

L'archive ouverte pluridisciplinaire **HAL**, est destinée au dépôt et à la diffusion de documents scientifiques de niveau recherche, publiés ou non, émanant des établissements d'enseignement et de recherche français ou étrangers, des laboratoires publics ou privés.

Copyright

# Identification of sources of potential fields with the continuous wavelet transform: Application to self-potential profiles

Dominique Gibert and Marc Pessel

Géosciences Rennes - CNRS/INSU, Université Rennes 1, France

## Abstract.

We show how the continuous wavelet transform may be used to quickly localize and characterize the sources of self-potential anomalies. The method is applied to synthetic examples and to a self-potential profile crossing a shallow fault zone.

## Introduction

Self-potential data carry unique information concerning fluid flows underground, geothermal and electrochemical phenomena [Corwin, 1990, Zhdanov and Keller, 1994]. Despite potential data are acquired since several decades only a few studies concern inversion [Fitterman and Corwin, 1982; Patella, 1997; Lapenna et al., 2000], and most studies use a forward approach and numerical modeling [Fitterman, 1978, 1979, 1983; Sill, 1983; Yasukawa et al., 1993; Wurmstich and Morgan, 1994; Michel and Zlotnicki, 1998; Adler et al., 1999; Jouniaux et al., 1999]. In the same spirit, recent studies concerning hydrological applications fit the data through hydro-dynamical models which ensure the physical coherence of the current sources responsible for the observed self potential [Ishido and Pritchett, 1999; Revil et al., 1999]. It might be useful to dispose of a less specialized (i.e. not assuming an hydrological origin for the sources) method to perform a rapid analysis of the data in order to obtain information (e.g. number of sources, depth range, multipolar nature, etc.) concerning the sources and which could be used as prior model for more sophisticated inversion methods [e.g. Patella, 1997; Lapenna et al., 2000]. In recent studies, we presented a theoretical framework based on the continuous wavelet transform which allows a quick analysis of potential field data [Moreau et al. 1997, 1999], and we show how this method can be used with self-potential data.

## Theoretical Background

The starting equation is the first-order (Born approximation) coupling equation between primary and secondary induced flows [Sill, 1983],

Copyright 2001 by the American Geophysical Union.

Paper number 2000GL012041.  
0094-8276/01/2000GL012041\$05.00

$$\vec{J}_{total} = -\eta \vec{Q} - \sigma \vec{\nabla} \phi, \quad (1)$$

where  $\vec{Q}$  is the primary flow (fluid flow, heat flux, etc.),  $\eta$  is the cross-coupling coefficient,  $\sigma$  is the electrical conductivity, and  $\phi$  is the electrical potential. The electrical current  $\vec{J}_{total}$  is the sum of the advective current,  $\vec{J}_{advec} = -\eta \vec{Q}$  created by the primary flow, and of the conductive current  $\vec{J}_{conduc} = -\sigma \vec{\nabla} \phi$  resulting from Ohm's law. If no external current sources exist and either the stationary regime approximation or the less restrictive quasi-static approximation holds, the total current flow is divergence-less,  $\vec{\nabla} \cdot \vec{J}_{total} = 0$ , and equation (1) gives:

$$\vec{\nabla} \cdot (\sigma \vec{\nabla} \phi) = \vec{\nabla} \cdot (-\eta \vec{Q}). \quad (2)$$

For constant electrical conductivity, equation (2) may be further simplified,

$$\nabla^2 \phi = \vec{\nabla} \cdot (-\beta \vec{Q}), \quad (3)$$

where  $\beta = \eta/\sigma$  is the voltage coupling coefficient. The source term of the Poisson equation (3) may be split as

$$\vec{\nabla} \cdot (-\beta \vec{Q}) = -\vec{\nabla} \beta \cdot \vec{Q} - \beta \vec{\nabla} \cdot \vec{Q}, \quad (4)$$

where the first right-hand term represents sources located where the primary flow crosses (almost perpendicularly) spatial variations of the coupling coefficient, and the second right-hand term represents external sources of primary flow (e.g. well pumping, rainfall, etc.).

The second mathematical item of the present study is the continuous wavelet transform of a function  $\phi_0$  which may be written as the convolution product,

$$\mathcal{W}[g, \phi_0](b, a) \equiv (\mathcal{D}_a g * \phi_0)(b), \quad (5)$$

where  $g$  is the analyzing wavelet, and  $\mathcal{D}_a$  is the dilation operator such that

$$\mathcal{D}_a g(x) \equiv \frac{1}{a} g\left(\frac{x}{a}\right), \quad (6)$$

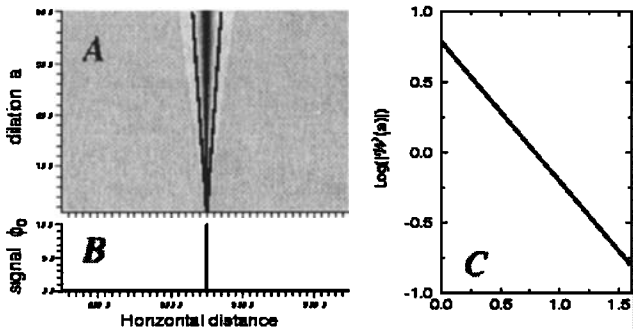


**Figure 1.** A: Continuous wavelet transforms of a Dirac impulse (B) of homogeneity  $\alpha = -1$ . The wavelet transform displays a cone-like geometry and the magnitude along any straight line crossing the cone apex varies according to a power law with exponent  $\alpha$  (C).

where the dilation  $a > 0$ . The analyzing wavelet is an oscillating localized function (i.e. with a compact or quasi-compact support) with a vanishing integral. The useful mathematical property concerns the geometrical structure of the wavelet transform of homogeneous functions  $\phi_0$  verifying

$$\phi_0(\lambda x) = \lambda^\alpha \phi_0(x), \tag{7}$$

with  $\alpha$  the homogeneity degree. Equation (5) gives:

$$\mathcal{W}[g, \phi_0](\lambda b, \lambda a) = \lambda^\alpha \mathcal{W}[g, \phi_0](b, a), \tag{8}$$

and the whole wavelet transform of the homogeneous function may be extrapolated from the wavelet transform given at a single dilation. The geometrical translation of this property is that the wavelet transform of an homogeneous function possesses a cone-like structure converging at the homogeneity center of the analyzed function (Figure 1). Also, the variation of the magnitude of the wavelet transform along any straight line crossing the homogeneity center is a power law of exponent  $\alpha$  with respect to  $a$  (Figure 1C) [Alexandrescu et al., 1995, 1996; Holschneider, 1995].

The continuation property (8) of the wavelet transform has been generalized, and a particular class of wavelets exists such that the wavelet transform of a potential field satisfying the Poisson equation (3) may be used to detect, localize and characterize homogeneous singularities present in the causative source distribution [Moreau et al., 1997, 1999; Hornby et al., 1999; Sailleac et al., 2000]. The main difference with respect to the analysis shown in Figure 1 is that the apex of the cone-like structure of the wavelet transform is no more located on the  $a = 0$  line, but now at  $a = -z_s$  below the wavelet half-plane,  $z_s$  being the depth of the causative source (Figure 2A). Applying a proper scaling of the dilations  $a$  with respect to  $z_s$  [Moreau et al., 1997, 1999] the power-law variation of the magnitude of the wavelet transform is restituted and the homogeneity degree  $\alpha$  of the source can be determined (Figure 2d,f). Hence, the wavelet transform gives both the location and the

nature (e.g. bipolar) of a singular source from its potential field anomaly (gravity, magnetic, self-potential). This mathematical framework constitutes a means to quickly analyze potential field data by representing the observed field in terms of homogeneous sources. This is not an inversion method but, instead, a pre-processing which may provide prior information useful for a more sophisticated inversion.

### Synthetic Examples

We now illustrate the method with two synthetic examples. The first one, whose results are shown in the top part of Figure 3, corresponds to a model of constant conductivity  $\sigma = 10^{-2} \text{ S.m}^{-1}$  with two current source points:  $x_s = 90 \text{ m}, z_s = 14 \text{ m}, \nabla \cdot \vec{J}_{advec} = -0.4 \text{ A.m}^{-3}$  and  $x_s = 110 \text{ m}, z_s = 12 \text{ m}, \nabla \cdot \vec{J}_{advec} = +0.4 \text{ A.m}^{-3}$ . The resulting potential (labelled a) has a wavelet transform (labelled b) with a clear cone-like structure whose apex is located in the  $(x_s, z_s)$  half-space by assessing the cone-like geometry of the wavelet transform with respect to every point in a rectangular domain of the  $(x_s, z_s)$  domain. In practice, the cone-like coherency is quantified by rescaling the wavelet transform with respect to the tested apex and by computing the slope of the wavelet transform modulus along a set of straight lines emerging from the tested apex. A normalized histogram  $h_i$  with  $N$  bins of the slopes  $p_j$  is computed and its  $\delta$ -like behavior is quantified by the following index based on Shannon entropy [Tass et al., 1998]

$$\rho(x_s, z_s) \equiv \frac{\ln N + \sum_{i=1}^N h_i \ln h_i}{\ln N}. \tag{9}$$

The index  $\rho$  varies from 0 for a uniform histogram to 1 for a  $\delta$ -like histogram. For this first example, the  $\rho(x_s, z_s)$  map (labelled c in the top part of Figure 3) indicates a narrow area for the source position with the

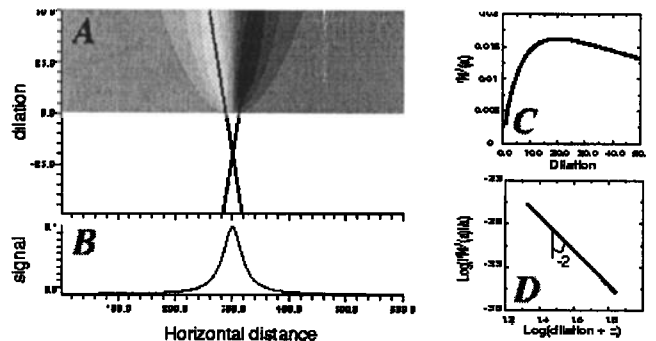


**Figure 2.** A: Continuous wavelet transform the potential field (B) caused by a bipolar source of homogeneity  $\alpha = -2$ . The apex of the cone is located at a negative dilation corresponding to the depth  $z_s$  of the source. C: The magnitude along any straight line crossing the cone apex now varies in a complicated manner. D: The power-law behavior is restituted when the dilation axis is properly rescaled with respect to  $z_s$ .

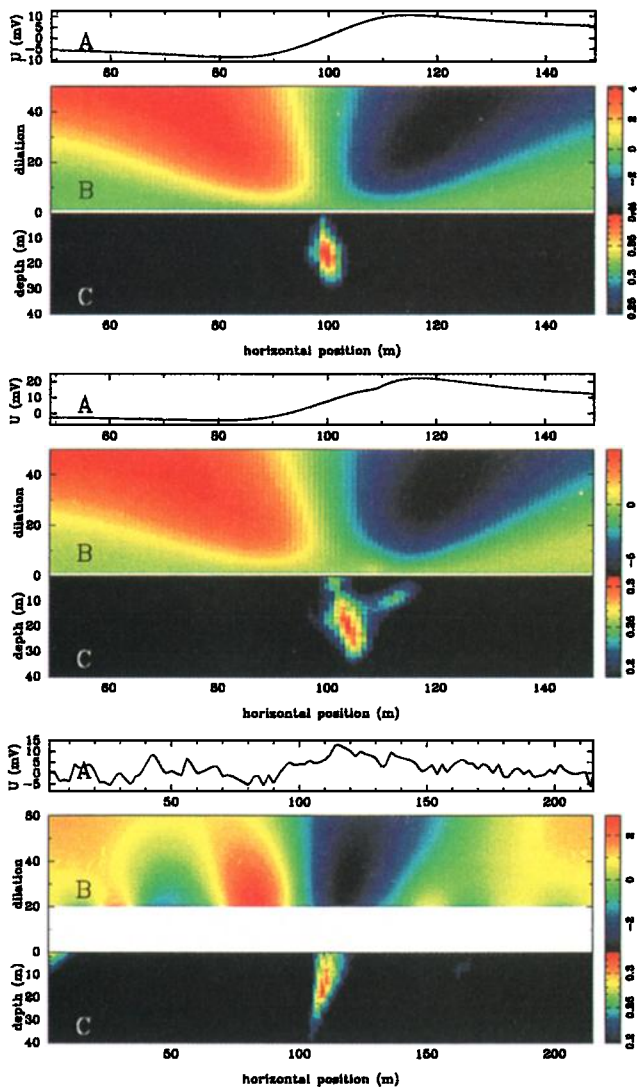


**Figure 3.** Top: Synthetic model with a constant conductivity  $\sigma = 10^{-2} \text{ S.m}^{-1}$ . A) potential created by two current source points  $x_s = 90 \text{ m}$ ,  $z_s = 14 \text{ m}$ ,  $I = -0.4 \text{ A.m}^{-3}$ , and  $x_s = 110 \text{ m}$ ,  $z_s = 12 \text{ m}$ ,  $I = +0.4 \text{ A.m}^{-3}$ . B) Continuous wavelet transforms of the potential profile. C) Map of the  $\rho$  measure showing the area where the cone-like structure of the wavelet transform is coherent. Middle: Same as above but for  $\sigma = 10^{-2} \text{ S.m}^{-1}$  left of  $x = 108 \text{ m}$  and  $\sigma = 2.10^{-3} \text{ S.m}^{-1}$  on the right. Bottom: A) Self potential along an east-west profile perpendicular to the Pont-Péan fault zone. The fault is approximately located at the  $x = 100 \text{ m}$  horizontal position and is inclined toward the left (eastward) with an angle of about  $80^\circ$ . B) Continuous wavelet transform of the data. The small-dilation range  $a < 20$  has been removed because of a too bad signal-to-noise ratio. C) Map of the  $\rho$  measure showing the most likely position of the current sources.

best location being  $x_s = 100 \text{ m}$  and  $z_s = 15 \text{ m}$  with an homogeneity degree  $\alpha = -2.05$  indicating a bipolar source. The depth to the source is slightly overestimated because the two current source points are actually separated by a finite distance  $\delta x_s = 20 \text{ m}$ .

The second example has the same current sources as the first one and a conductivity structure with two blocks of different conductivities separated by a vertical fault plane located at  $x = 108 \text{ m}$ . The results are shown in the middle part of Figure 3 and, as expected, the location of the current sources is not so accurate as in the first example since the constant-conductivity assumption of equation (3) is not valid. This results in a horizontal location  $x_s = 104 \text{ m}$  of the equivalent bipolar source biased toward the less conductive block, and  $z_s = 18 \text{ m}$ . Despite these perturbations, the homogeneity degree remains unchanged,  $\alpha = -2.07$ , still indicating a bipolar current source.

### Analysis of the Pont-Péan Data

The Pont-Péan fault-zone is a mineralized diorite dike which has been industrially exploited during the 18th and 19th centuries until a massive flood invaded the underground galleries in April 1904. The area has been extensively prospected and the geological structure is well-known, with a linear 4 km-long fault which enables a very good 2D approximation. Although located in the Pont-Péan village 10 km south of Rennes (Britanny, France), the area is not industrialized and the geophysical measurements are of good quality (i.e., good signal-to-noise ratio and repeatability of measurements). The electrical potential measured perpendicularly to the fault is shown in the bottom part of Figure 3 and display a bipolar anomaly located in the vicinity of the fault zone. The dilation range  $a < 20$  of the wavelet transform was not considered because of a too low signal-to-noise ratio (see *Alexandrescu et al.* [1995] for details concerning the wavelet transform of noisy signals). However, the cone-like structure of the wavelet transform is conspicuous and the location area of the source obtained from the  $\rho$  map is rather limited in extend with a clearly marked maximum centered at  $x_s = 107 \text{ m}$ ,  $z_s = 15 \text{ m}$  with an homogeneity degree  $\alpha = -2.25$  very near the one of a pure bipolar source. The shallow depth to the source indicates that the self-potential signal is more likely produced by shallow fluid flow in the fault zone rather than by electro-chemical phenomena arising in the mineralized dike whose top has been found much deeper (i.e.  $> 80 \text{ m}$ ). This result agrees with a recent electrical impedance tomography performed along the same profile [*Pessel and Gibert*, 2001] which indicates that the electrical sources identified in the present study are localized in a highly conductive zone located above the fault zone and probably associated with very altered rocks.

### Conclusion

In this letter, we show how the continuous wavelet transform may be used to analyze self-potential data. Straightforward application to 3D cases is possible provided potential data acquired in the  $(x, y)$  plane are

available. The theoretical framework established by Moreau *et al.* [1997, 1999] may formally be applied only if the electrical conductivity is a constant. However, the synthetic example corresponding to the inhomogeneous conductivity model (middle part of Figure 3) shows that the theory may still be applied with an acceptable accuracy level. The wavelet analysis provides both an estimate of the location and of the nature (dipole, etc.) of the current source responsible of a given self-potential signal. This may constitute a prior information useful to initiate a more sophisticated inversion strategy like the one recently proposed by Patella [1997]. It must be kept in mind that the sources identified by the wavelet method proposed in the present paper are homogeneous (e.g. bipolar) and constitute the simplest source model obtained from the information contained in the potential data alone. More physically realistic sources could subsequently be derived by replacing the localized homogeneous sources by extended ones producing the same multipolar potential fields (e.g. a sphere is equivalent to a monopolar source). However, this may be achieved only at the expense of additional information as shown in the paper by Sailhac and Marquis [2000] which uses hydrological constraints (e.g. continuity equation) together with potential field data.

**Acknowledgments.** We thank Georges Ruelloux and Aude Chambodut for kind assistance during the field operations, and the Galène association (<http://pont-pean-le-village.com>) for both historical and geological informations concerning the Pont-Péan mining industry. André Revil made a very constructive review. This work is financially supported by the CNRS and ANDRA through the GdR FORPRO (Research action number 99.II) and corresponds to the GdR FORPRO contribution number 2000/34A. This study is a part of the Electrical Tomography Project of the CNRS ACI *Eau et Environnement*.

## References

- Adler, P.M., J.-L. Le Mouél, and J. Zlotnicki, Electrokinetic and magnetic fields generated by flow through a fractured zone: A sensitivity study for La Fournaise volcano, *Geophys. Res. Lett.*, *26*, 795-798, 1999.
- Alexandrescu, M., D. Gibert, G. Hulot, J.-L. Le Mouél, and G. Saracco, Detection of geomagnetic jerks using wavelet analysis, *J. Geophys. Res.*, *100*, 12557-12572, 1995.
- Alexandrescu, M., D. Gibert, G. Hulot, J.-L. Le Mouél, and G. Saracco, Worldwide wavelet analysis of geomagnetic jerks, *J. Geophys. Res.*, *101*, 21975-21994, 1996.
- Corwin, R.F., The self-potential method for environmental and engineering applications, in *Geotechnical and Environmental Geophysics*, 127-146, S.H. Ward ed., SEG, 1990.
- Fitterman, D.V., Electrokinetic and magnetic anomalies associated with dilatant regions in a layered Earth, *J. Geophys. Res.*, *83*, 5923-5928, 1978.
- Fitterman, D.V., Calculations of self-potential anomalies near vertical contacts, *Geophysics*, *44*, 195-205, 1979.
- Fitterman, D.V., Modeling of self-potential anomalies near vertical dikes, *Geophysics*, *48*, 171-180, 1983.
- Fitterman, D.V., and R.F. Corwin, Inversion of self-potential data from the Cerro Prieto geothermal field, Mexico, *Geophysics*, *47*, 938-945, 1982.
- Holschneider, M., *Wavelets: An Analysis Tool*, 423 pp., Clarendon, Oxford, England, 1995.
- Hornby, P., F. Boschetti, and F.G. Horowitz, Analysis of potential field data in the wavelet domain, *Geophys. J. Int.*, *137*, 175-196, 1999.
- Ishido, T., and J.W. Pritchett, Numerical simulation of electrokinetic potentials associated with subsurface fluid flow, *J. Geophys. Res.*, *104*, 15247-15259, 1999.
- Jouniaux, L., J.-P. Pozzi, J. Berthier, and P. Massé, Detection of fluid flow variations at the Nankai Trough by electric and magnetic measurements in boreholes or at the seafloor, *J. Geophys. Res.*, *104*, 29293-29309, 1999.
- Lapenna, V., D. Patella, and S. Piscitelli, Tomographic analysis of self-potential data in a seismic area of Southern Italy, *Annali di Geofisica*, *43*, 361-373, 2000.
- Michel, S., and J. Zlotnicki, Self-potential and magnetic surveying of La Fournaise volcano (Réunion island): Correlation with faulting, fluid circulation, and eruption, *J. Geophys. Res.*, *103*, 17845-17857, 1998.
- Moreau, F., D. Gibert, M. Holschneider, and G. Saracco, Wavelet analysis of potential fields, *Inverse Probl.*, *13*, 165-178, 1997.
- Moreau, F., D. Gibert, M. Holschneider, and G. Saracco, Identification of sources of potential fields with the continuous wavelet transform: Basic theory, *J. Geophys. Res.*, *104*, 5003-5013, 1999.
- Patella, D., Introduction to ground surface self-potential tomography, *Geophys. Prospecting*, *45*, 653-681, 1997.
- Pessel, M., and D. Gibert, Multiscale electrical impedance tomography, *J. Geophys. Res.*, *106*, in press, 2001.
- Revil, A., H. Schwaeger, L.M. Cathles III, and P.D. Manhardt, Streaming potential in porous media 2. Theory and application to geothermal systems, *J. Geophys. Res.*, *104*, 20033-20048, 1999.
- Sailhac, P., and G. Marquis, Analytic potentials for the forward and inverse modeling of SP anomalies caused by subsurface fluid flow, *Geophys. Res. Lett.*, in press, 2001.
- Sailhac, P., A. Galdeano, D. Gibert, F. Moreau, and C. Delor, Identification of sources of potential fields with the continuous wavelet transform: Complex wavelets and application to aeromagnetic profiles in French Guiana, *J. Geophys. Res.*, *105*, 19455-19475, 2000.
- Sill, W.R., Self-potential modeling from primary flows, *Geophysics*, *48*, 76-86, 1983.
- Tass, P., M.G. Rosenblum, J. Weule, J. Kurths, A. Pikovsky, J. Volkmann, A. Schnitzler, and H.-J. Freund, Detection of  $n:m$  phase locking from noisy data: Application to magnetoencephalography, *Phys. Rev. Lett.*, *81*, 3291-3294, 1998.
- Wurmstich, B., and F.D. Morgan, Modeling of streaming potential responses caused by oil well pumping, *Geophysics*, *59*, 46-56, 1994.
- Yasukawa, K., G.S. Bodvarsson, and M.J. Wilt, A coupled self-potential and mass-heat flow code for geothermal applications, *Trans. Geotherm. Resour. Council.*, *17*, 203-207, 1993.
- Zhdanov, M.S., and G.V. Keller, *The Geoelectrical Methods in Geophysical Exploration*, Elsevier, New York, 1994.

D. Gibert, Géosciences Rennes, Université Rennes 1, Bât. 15 Campus de Beaulieu, 35042 Rennes cedex, FRANCE. (e.mail: gibert@univ-rennes1.fr)

M. Pessel, CEREGE, Europôle Méditerranéen de l'Arbois, BP 80, 13545 Aix-en-Provence cedex 04, FRANCE. (e.mail: pessel@cerege.fr)

(Received July 12, 2000; revised January 22, 2001; accepted January 30, 2001.)